Proceedings of Global Power and Propulsion Society
ISSN-Nr: 2504-4400
GPPS Hong Kong 2023
October 17-19, 2023
www.gpps.global

GPPS-TC-2023-0175

Aeroacoustic Performance Comparison Between a Small Contra-Rotating Fan and the Series Operation of Two Fans

Tianyu Xu
Department of Mechanical Engineering, The University of Hong Kong
Tianyu30@connect.hku.hk
Pokfulam Road, Hong Kong SAR, China

Bin Dong*(Corresponding)
High-Speed Aerodynamics Institute, China Aerodynamics Research and Development Center
nudt18214@163.com
Mianyang, Sichuan, China

Dangguo Yang
High-Speed Aerodynamics Institute, China Aerodynamics Research and Development Center
yangdg-cardc@163.com
Mianyang, Sichuan, China

Ronghui Ning
High-Speed Aerodynamics Institute, China Aerodynamics Research and Development Center
nrhui09@cardc.cn
Mianyang, Sichuan, China

ABSTRACT

Small axial flow fans are frequently used as air coolers or ventilators, and their aeroacoustic mechanism is similar to those found in larger machinery like aeroengines. Currently, there is a growing interest in adopting contra-rotation due to its inherent aerodynamic advantages. However, acoustically, contra-rotating (CR) fans radiate additional interaction noise, which decreases the sound quality and may cause extra annoyance. In this work, a sample CR fan is designed using simple radial equilibrium theory supplemented by three-dimensional steady-flow simulations, and its aeroacoustic performance is compared with that of two fans in a series. In general, the designed CR fan can produce a larger volumetric flow rate as well as a higher total pressure rise at lower rotational speeds compared with the series design. An acoustic comparison of specific noise levels shows that, in the flow rate range from the design point to higher flow rates, the CR fan is quieter. However, when the CR fan stalls in the lower flow rate region, its specific noise level is higher than that of the fan series. In addition, from the noise spectrum, the tonal noise power of the CR fan is less than that of the fan series.

Keywords: contra-rotating fan; series operation of two fans; specific noise level; interaction noise.

NOMENCLATURE

CR	Contra-rotating
CROR	Contra-rotating open rotor
BPF	Blade passing frequency
HVAC	Heating, ventilation, and air conditioning
rpm	Revolutions per minute
SPL	Sound pressure level
SPLA	A-weighting sound pressure level
PSD	Power spectral density

INTRODUCTION

There has been a continuing attempt to apply contra-rotation to axial flow work-absorbing turbomachines in open or closed configurations (Peake and Parry, 2012; Mitchell and Mikkelson, 1982; Dong et al., 2020). The former refers to rotors that are not utilized together with a casing or housing, such as contra-rotating (CR) propellers and open-rotor engines (CROR). In contrast, the latter refers to CR fan or compressors that have rotors enclosed within a casing. The two conventional fans in the series are similar to the CR fan in structure, which will cause a nearly double pressure rise and can overcome the relatively higher system impedance than fans in parallel. Therefore, two fans in the series can approximately imitate the same working state as the CR fan under normal working conditions and this comparison makes sense to some

extent. By comparing with the conventional fan series, the acoustic properties of CR fan need to be highlighted, which is also the purpose of this paper.

The current effort is focused on small CR fan that operate in the low-speed domain because there has not been much research in this area. Small fans are typically incompressible turbomachines, which are frequently used in HVAC (heating, ventilation, and air conditioning) systems as air coolers or ventilators. To produce a high-pressure rise or a larger flow rate, respectively, several small fans can be practically set up to operate in series or parallel (Jorgenson, 1999; Wang, 2018). A higher flow rate can remove more heat through airflow, and a higher pressure increase is desirable for overcoming the resistance of the system. Due to weight and dimension limitations in a particular HVAC system, the conventional combination of two fans would not be satisfactory. Small CR fan are highly specialized for situations where it is nearly impossible to simultaneously achieve a higher pressure rise and a larger flow rate. Only a selected few of the works towards small fans are given here: Hot-wire measurements were taken by Cho et al. (2009) to examine the 3D unsteady flow field in a low-speed CR fan (tip velocity U_t = 45.8 m/s) upstream, downstream, and between the rotors. It was discovered that the three velocity components showed more periodic characteristics in the mean-radius region than in the hub region, that the axial velocity component in the tip region was significantly reduced as a result of the effects of the casing boundary and the tip leakage flow, and that the radial and tangential velocity components experienced more unsteadiness than the axial component. Shigemitsu et al. (2013) then proceeded to analyze the internal flow condition of a small-sized CR fan (40 mm in diameter). They highlighted that for both the front and rear rotors, there were significant back-flow zones close to the shroud as a result of the axial pressure gradient of each rotor, which needed to be addressed for further improvement in fan performance. Wang et al. (2013) conducted comparison studies comparing single-rotor, rotor-stator, and CR fan (380 mm in diameter) in terms of fan overall performance and wall pressure fluctuations. The CR fan was shown to have more operational stability, static pressure rise, and aerodynamic efficiency than single-rotor and rotor-stator fans. These studies give us the foundation that we need to understand the aerodynamic characteristics of small CR fan. To obtain a fair comparison, two small conventional fans are designed to operate in series with the CR fan configured with two rotors in the stage.

In recent years, research on CROR has also been a popular topic in terms of their noise attenuation. Chaitanya et al. (2022) performed a detailed experimental study of the contra-rotating propeller of co-axis configuration under the hover condition with tip Mach number 0.2. They investigated the sensitivity of radiated noise to axial separation distance using a thorough statistical investigation and found the optimum separation distance of one-quarter of the diameter of the propeller where the minimum noise level was measured. Additionally, it is demonstrated that the distance with the lowest radiated noise also obtains the best aerodynamic performance. Blade modifications are also good ways to suppress the noise of enclosed duct contra-rotating fans. Krause et al. (2019) introduced a technique known as rotational beamforming that enables the virtual rotation of the microphones to detect sound sources on the rotating blades with modifications on both the leading edge and the trailing edge. They proved that the noise radiation could be decreased by using the serration at the trailing edge. The following part will mainly introduce the comparison and analysis of the experimental results of the contra-rotating fan and two series of small axis-flow fans.

RESEARCH CONFIGURATIONS

Multiple-fan combinations are commonly used in the industry, which include the fan series and parallel fan operation. For the parallel fan, the airflow rate is almost doubled with no resistance in the system, but the pressure of it is still the same as a single fan. However, for the fan series, the static pressure is nearly doubled while the airflow rate has no obvious change. The CR fan brings together the best of both, which not only has the double pressure rise but the double flow rate as well. In general, the fan in the series is normally chosen to substitute the single fan due to its higher pressure rise to overcome the resistance of the system, which the CR fan can also do the same. Besides, the CR fan looks like two fans in a series with similar structural sizes in terms of appearance. Therefore, the comparison of the conventional fans in series and the CR fan will be the focus of this paper. Specific details will be introduced in the following sections.

Two conventional fans in a series

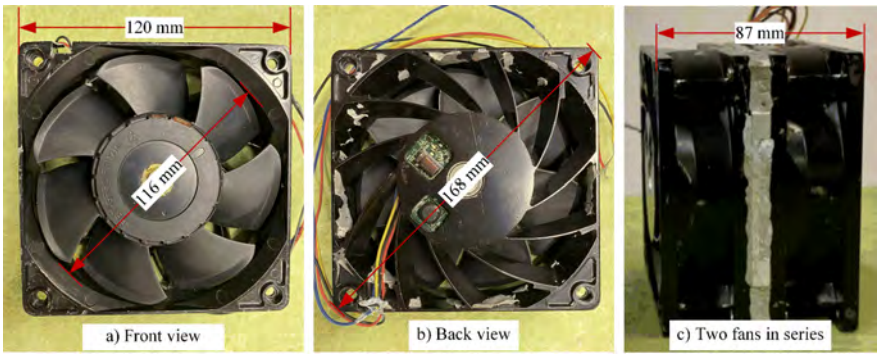

Figure 1 Configuration of the conventional fan and two fans in series

The conventional fan features a rotor-stator structure and is mainly used for data server cooling. In this paper, the fan series will be mounted with a circular flange on the test rig. There are seven blades and 12 vanes for the rotor and stator, respectively. The conventional fan has a square frame with a side length of 120 mm and an axial length of 40 mm. The radius of the circular flow passage inside the square frame is 116 mm. Two conventional fans are used in series to produce a higher pressure rise and a larger volumetric flow rate. In this situation, the axial length increases to 87 mm. Since there is no aerodynamic coupling between the two conventional fans, which is just a simple superposition, there is no special regulation on the distance between the two fans. Figure 1 shows the configuration of the conventional fan. The detailed parameters of the fan series are listed below:

Table 1 The detailed parameters of the conventional fan series combined by two same fans

Parameters	Fan series
Hub radius r_h (mm)	31.5
Tip radius r_t (mm)	56.8
Frame inner radius r_d (mm)	58
Tip clearance ε (mm)	1.2
Axial chord length c_a (mm)	40
Blade number B	7
Designed Reynolds number	49119
Rotational speed (*rpm*)	3660
Shaft-rotation frequency f (Hz)	61

The investigated CR fan

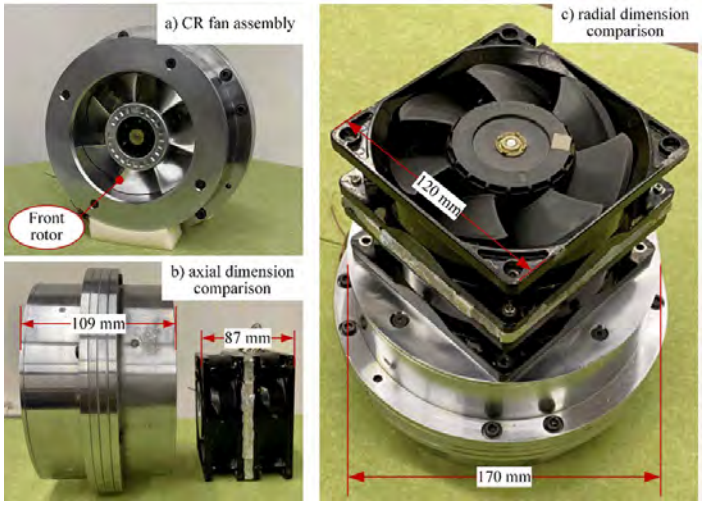

Figure 2 CR fan assembly and its dimensional comparison with conventional fans in series

A small CR fan of 116 mm in diameter is developed, referring to the dimensions of the above conventional fan, so they can be tested by the same test rig. The CR fan operates at standard atmospheric conditions, producing a total pressure rise ΔP_t of 150 Pa with a volumetric flow rate Q of 4 m^3/min. The rotational speed of the front rotor is N_1 = 3660 *rpm*

(revolutions per minute), and that of the rear rotor is $N_2 = 3180$ *rpm*. The inner radius of the casing r_d is set to be 116 mm, and the rotor tip radius r_t is 57.2 mm, resulting in a tip clearance $\varepsilon = r_d - r_t = 0.8$ mm. The hub radius for both rotors is $r_h =$ 31.5 mm, which is the same as that for the conventional fan. The blade numbers of the front and rear rotors are optimized to be $B_1 = 7$ and $B_2 = 5$, respectively, so that the efficient acoustic modes of interaction noise can be avoided. The axial spacing g_a between the trailing edge of the front rotor and the leading edge of the rear rotor is about 18.2 mm. It should be pointed out that the conventional fan has a tip clearance of 1.2 mm, which is about 1.5 times that of the small CR fan. The axial length of the CR fan is 109 mm, about 22 mm longer than that of two conventional fans in series. However, it is expected that the CR fan axial length can be further reduced when utilizing an integrated molding process to produce the CR fan frame; that is, the space used for screw joints can be saved. Figure 2 depicts the assembly of the small CR fan and its dimensional comparison with two conventional fans in series. The outer diameter of the CR fan frame d_o is defined as 170 mm based on the diagonal length of the square frame of the conventional fan. The intention is to see how much aeroacoustic gain can be obtained by contra-rotation when the CR fan and two conventional fans in the series have similar dimensions. The motors driving the front and rear rotors of the CR fan are the same as those of the conventional fan. The motor has an input voltage of 48 V. The main parameters of the small CR fan are further summarized in Table 2.

Table 2 The detailed parameters of the contra-rotating fan

Parameters	Front rotor	Rear rotor
Hub radius r_h (mm)	31.5	31.5
Tip radius r_t (mm)	57.2	57.2
Frame inner radius r_d (mm)	58	58
Tip clearance ε (mm)	0.8	0.8
Axial chord length c_{1a}, c_{2a} (mm)	24.5	30
Blade number B_1, B_2	7	5
Rotational speed N_1, N_2 (*rpm*)	3645	3165
Shaft-rotation frequency f_1, f_2 (Hz)	60.75	52.75

ANALYSIS AND COMPARISON

Test rig for two types of fans

As shown in Figure 3, the fan test rig is designed based on ANSI/AMCA Standard 210 (1999), which is one of the uniform methods of standard laboratory tests to measure the aerodynamic performance of target induced-flow fans. The investigated CR fan is installed at the inlet of the test rig, of which the diameter D = 120 mm is required to be the same as that of the fan casing or housing. A bell mouth is flushed-positioned at the fan inlet in order to reduce the distortion in the incoming flow. In addition, a flow straightener is mounted 3.5D downstream of the fan outlet, which aims to decrease the non-axial flow components so as to ensure more accurate measurement of static pressure and dynamic pressure by the Pitot tube which is located 5.2D downstream of the straightener. The throttling device is placed 3.8D downstream of the measurement point to adjust the back pressure, as thus, the mass flow rate will be changed under different working conditions.

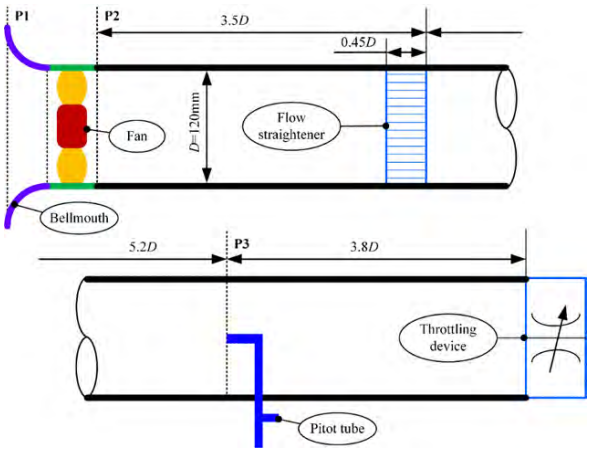

Figure 3 Test rig measuring the aerodynamic performance of small-sized fans

The flow straightener, which has several squared cells with dimensions of 0.45D in-depth, 0.075D inside length, and 0.005D in thickness, is detailed in Figure 4. The cell sides need to be flat, straight, and smooth. The Pitot tube then

measures the dynamic pressure P_{v3} and the total pressure P_{t3} locally at plane 3 (denoted as P3) (Dong, 2021). P3 has a rather reasonable velocity profile because it is far from the fan outlet and the flow straightener also smooths out the exit flow from the fan. In order to depict the average velocity of the profile for the measurement at P3, a single Pitot tube is used at a radial station. According to this, the total pressure at plane 2 (P2) is determined from that at P3, taking into account the pressure loss caused by the flow straightener and duct wall friction, with some empirical corrections recommended by the standard (AMCA, 1999). Specifically, the volume flow rate at the test point Q3 can be calculated via $Q_3 = v_3 A$. Here, A is the cross-section area of the test tube and v_3 can be obtained by the value of dynamic pressure. The gauge total pressure at the test point is also measured by the Pitot tube, which is the difference between the atmospheric pressure and absolute total pressure. In view of the existence of the straightener and duct wall friction, the gauge total pressure at the fan outlet can be calculated by (AMCA, 1999):

$$P_{t2}=P_{t3}+\frac{f(L_e+L_{23})P_{v3}}{D} \tag{1}$$

Here, f is the friction coefficient, L_e is the equivalent length of the straightener and L_{23} is the distance between P2 and P3. In general, a larger pressure loss will result from a higher flow velocity at P3.

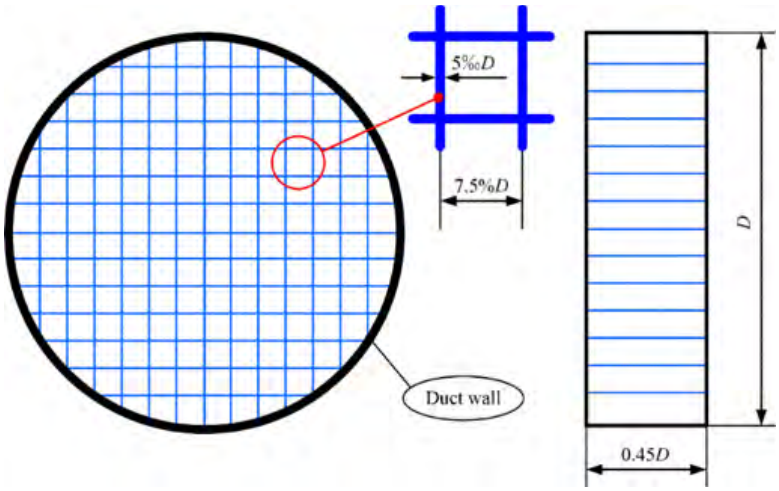

Figure 4 Geometrical features of the flow straightener

The far-field acoustic measurement is set up to test the noise of the fans, which are placed in an anechoic chamber and its cut-off frequency is 100 Hz. The fan is mounted at the inlet of the aerodynamic test apparatus, as shown in Figure 5. A B&K Nexus conditioning amplifier is used to supply four 1/4-inch microphones uniformly dispersed over a quarter-circle at four angle points 0.8 m horizontally apart from the fan's front rotor center. A 16-bit A/D card (NI USB-6251) is employed to sample the noise data at a frequency of 51.2 kHz, and the duration for each data acquisition at one measurement position is set to be 20 s. Signal processing is then conducted on a personal computer installed with the software MATLAB (Dong, 2023).

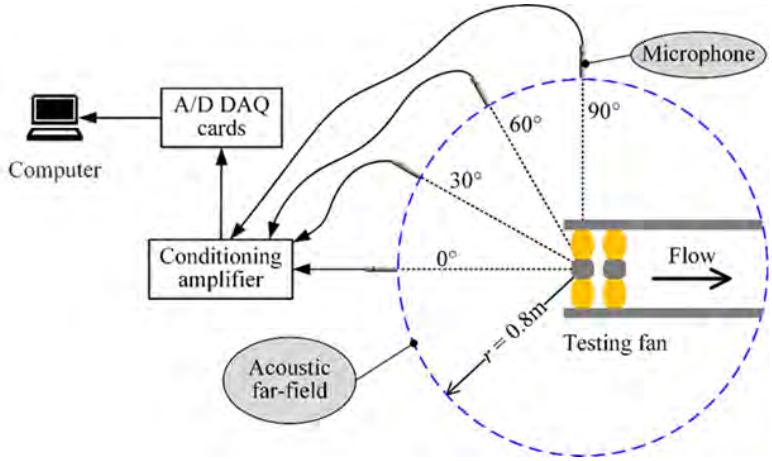

Figure 5 Acoustic performance measurement setup

Aerodynamic performance

The aerodynamic performance curves of the CR fan and two conventional fans in series are measured and compared. Two fans in series are operated at three operational conditions of different rotational speed combinations so as to demonstrate aerodynamic advantages achieved by contra-rotation with lower rotational speeds. The measurement scheme will be carried out according to the following four schemes:

Table 3. The test schemes of the fans

Test Schemes	Rotating Speed (*rpm*)			
	CR fan		Fan series	
	Front	Rear	Front	Rear
CR	3180	3660		
SO1			3180	3660
SO2			4990	4990
SO3			4560	4560

In series operation 1 (SO1), the rotational speeds of the front and rear fans are 3180 *rpm* and 3660 *rpm*, respectively, being the same as those of the CR fan. However, the speeds need to be increased to about 4990 *rpm* in SO2 in an effort to match the CR fan design point (denoted as a green rhombus ◇). In practice, a flow straightener or a net screen is usually installed in the interstage space of the series operation for the purpose of reducing flow distortions to the rear fan. Such treatment considerably improves the aerodynamic performance of the series operation of conventional fans. By doing this to match the CR fan design point, the speeds of the front and rear fans in SO3 need to be increased to about 4560 *rpm*, which is 430 *rpm* lower than that of SO2 but still much higher than those of the CR fan. In either condition, the series operation faces much higher rotational speeds to gain the same aerodynamic performance as the CR fan, particularly in the relatively high flow rate range around its design point. The comparison is shown in Figure 6.

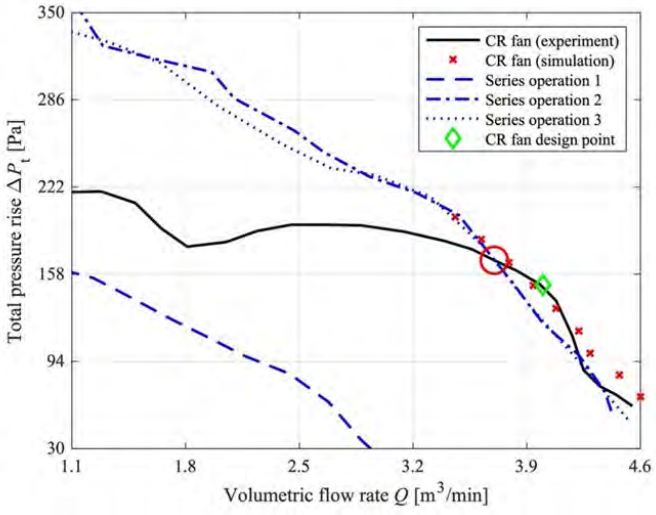

Figure 6 Aerodynamic performance comparison between the designed CR fan and the series operation of two industrial fans

In comparison to the performance curve of the CR fan, SO1 presents a much lower but typically steeper curve, implying a smaller total pressure rise with a narrower flow rate range. Moreover, for all the series operation conditions, an approximately proportional relationship between total pressure rise and volumetric flow rate can be found. However, this is not the case with the small CR fan, and its performance curve presents different variation trends in the flow rate range. To be specific, to the right of the design point, the total pressure rise of the CR fan drops rapidly, thereby resulting in a curve segment with a relatively steep slope. In contrast, to the left of the design point till the flow rate point of 1.8 m^3/min, the curve experiences mild variations of total pressure rise, presenting a broad hump in this range. However, the CR fan performance curve starts to climb again in the flow rate range after the hump. When the rotational speeds of SO2 and SO3

reach 4990 *rpm* and 4560 *rpm*, respectively, their aerodynamic performances are nearly identical throughout the flow rate range and are particularly able to compete with the CR fan performance in the range around the design point. It is therefore suggested that for a given operating point, the rotational speeds of a small CR fan could be significantly lower than those of conventional fans in series operation. This is attributed to the aerodynamic advantages of contra-rotation. In light of the reduced speeds of the CR fan, some acoustic benefits are possible.

Acoustic performance

In this part, the specific noise level K_s is introduced to determine the noise rating of fans with different configurations. It is defined as (Fukano et al., 1986):

$$K_s = SPLA - 10log_{10}\left(\frac{Q\Delta P_t^2}{W_{ref}}\right) \tag{2}$$

where the units of the fan flow rate Q and total pressure rise ΔP_t are m^3/s and kp/m^2 (kilopond per square meter), respectively, and the reference quantity W_{ref} is 1 $kp^2/(m \cdot s)$. The fan sound pressure level with A-weighting (SPLA) is normalized by the aerodynamic outputs. As a result, the noise radiation of different fan types can be compared in the parametric space of pressure rise versus flow rate.

The noise levels of several fan types are compared in Figure 7 as a function of the volumetric flow rate. A green rhombus (◇) denotes the design point of the CR fan. The U-shape distribution of the specific noise level may be noticed in all fan types. The designed CR fan is the quietest in the flow rate range surrounding its design point and from this point to higher flow rates. The specific noise level of the CR fan is marginally lower than that of series operation 2 without an interstage net screen in the range with mid-flow rates (from 2.67 m^3/min to 3.71 m^3/min), while series operation 3 with a net screen is the quietest. The CR fan is observed to stall below the flow rate threshold at 2.67 m^3/min, and from this point to lower flow rates, its specific noise level is the greatest of all fan kinds. The aerodynamic coupling in the stage is prone to break in the stall condition because the CR fan runs in an unstable state with a higher flow resistance, which prevents the rear rotor from effectively recovering the remaining swirls from the front rotor. Series operations 2 and 3 with faster rotational speeds, however, are both substantially quieter and simultaneously create a greater total pressure rise than the CR fan in the range with relatively lower flow rates. It follows that the CR fan performs better than the fan series in the range of mid-to-high flow rates, where its advantage in aeroacoustics can be discovered. In this flow rate range, the CR fan operating at lower rotational speeds is more environmentally friendly (lower specific noise levels) and energy-efficient (lower rotational speeds) than the industrial fans operating in series.

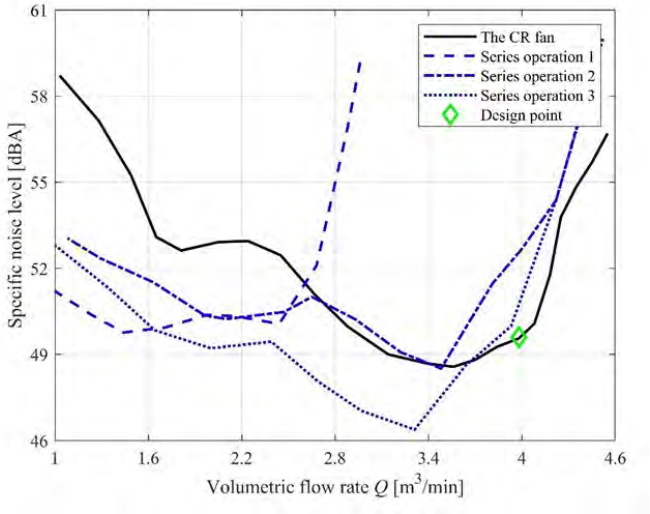

Figure 7 Specific noise level comparison between the CR fan and the series operation of two industrial fans

In addition, the measured noise signal is also processed with the MATLAB *pwelch* function to get the power spectral density (PSD) and based on it, the sound pressure level (SPL) can be calculated. The SPL spectrum, on the other hand, is ineffective for visualizing the acoustic energy distribution over frequencies or the intensity of tonal components embedded in the spectrum. Thus, the cumulative sound power can be applied in this case, which is defined as the integration of the power spectral density from the frequencies f_L to f_i in the form of (Lee and Bolton, 2016):

$$\mathcal{P}(f_i) = \int_{f_L}^{f_i} \frac{p^2(f)}{\rho_0 c_0} df \tag{3}$$

where $p^2(f)$ is obtained through the *pwelch* function, ρ_0 is the air density and c_0 is the speed of sound. The slope of the equation indicates the degree of the acoustic energy concentrates for the spectrum. The SPL and cumulative sound power spectra at the common aerodynamic power point (marked with a red circle ○ in Figure 6) are illustrated in Figure 8 below.

The noise spectra in the frequency range from 50 Hz to 8000 Hz of the CR fan (black solid line) and SO3 fan series (blue dashed line) are depicted in the upper half part of Figure 8, which is presented on a logarithmic scale with a resolution of 1/48 octave band. The overall noise level of CR fan is about 61.47 dBA which is basically equal to that of the SO3 fan series with 61.59 dBA. It is obvious that from the frequency range 50 Hz to 3560 Hz, the broadband noise of the CR fan is generally higher than that of the fan series, and beyond this range the trend is the other way around. The remarkable tones generated by CR fan above 35 dBA are noted on the plot, which is related to the rotor-alone tonal noise and the interaction tonal noise of both. The BPFs of the front and rear rotor are denoted by f_1 and f_2 severally. The rotor-alone tones are composed of the integer multiples of either f_1 or f_2, while the frequencies of interaction tones are the linear combinations of each BPF. The important tones within the frequency range from 50 Hz to 2500 Hz are two rotor-alone tones of the second and the third harmonics of the rear rotor BPF and four interaction tones with mode order $|m| \leq 3$. The interaction tone frequency f_{in} and its circumferential mode m can be defined as (Wang and Huang, 2018):

$$f_{in} = \frac{1}{2\pi} |m_1 B_1 \Omega_1 - m_2 B_2 \Omega_2| \tag{4}$$

$$m = m_2 B_2 - m_1 B_1 \tag{5}$$

where m_1 and m_2 are integers, from $-\infty$ to $+\infty$, B is the blade number and Ω means the angular velocity of the rotor with the unit rad per second (rad/s). The signs of indices m_1 and m_2 must be the same, so that the mode order m at the frequency f_{in} has a much higher angular velocity than the relative angular velocity, allowing the mode to radiate efficiently. However, when m_1 and m_2 have the opposite sign, the mode will rotate at a rotational speed less than $\Omega_1 + \Omega_2$, resulting in relatively feeble radiation.

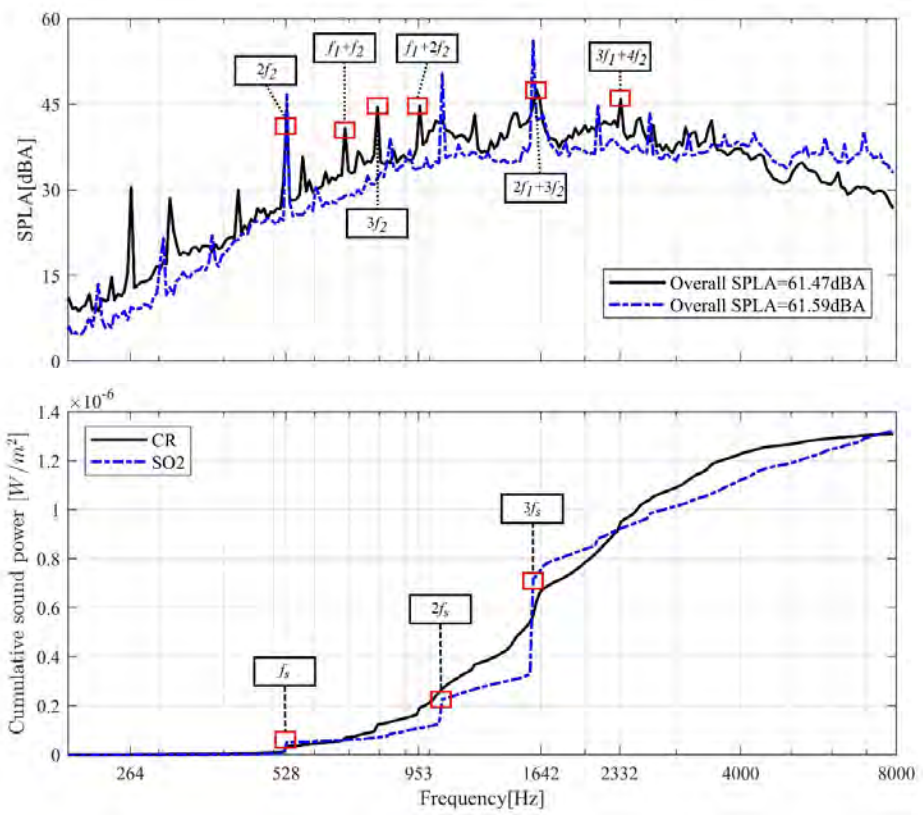

Figure 8 The noise spectra for the comparison of specific noise level and cumulative sound power between the CR fan and the fan series

The two curves in the lower half part of Figure 8 represent the cumulative sound power of the two fan types based on the 1/48 octave band plotted above, and f_s denotes the BPF of the fan series. The noise power distribution can be easily detected in this figure: for the CR fan, the tone at 528 Hz offers the first step of sound power due to the radiation of the rear rotor, and below this frequency point there is nearly no tonal contribution to the whole power. And from 528 Hz to

around 953 Hz, the slope of the curve is relatively lower than the slope in the range from 953 Hz to 2332 Hz, suggesting a larger sound power radiation among medium-high frequencies in terms of the CR fan than low or high frequency bands. The sound power contribution of the rotor-alone noise and interaction noise is obviously lower than the broadband noise which may be caused by the turbulence and flow distortion. Nevertheless, for the fan series, although the same step shows at 528 Hz due to its first BPF, the slope from this point to the higher frequency range is gentle and there is not much more broadband noise contribution than the CR fan. Then the steps for its curve all correspond to its BPFs (integer multiples of f_s). But at about 1570 Hz, a dramatic tonal noise of the fan series added to the noise power, which proves that the fan series with the same rotating speed will enhance noise radiation at BPFs. In general, from around 528 Hz to 1570 Hz, the sound power of the CR fan is higher than the fan series. Then a large step increase of the fan series results in a larger increase of sound energy than the CR fan from $3f_s$ to around 2310 Hz. Thus, the whole noise energy of the fan series exceeds the CR fan within this frequency range. At 8000 Hz, the final sound power of each fan type is nearly the same, which corresponds to approximately the same SPL value.

CONCLUSIONS

The series operation of small-sized axial flow fans and a contra-rotating fan are tested and compared by a designed test rig. For aerodynamic performance, the contra-rotating fan shows considerably greater efficiency than the series operation under the same rotating speed. The series operation requires significantly greater rotational speeds to provide the same aerodynamic performance as the CR fan, especially in the relatively larger flow rate range surrounding its design point. This is due to the aerodynamic benefits of contra-rotation. Because of the lower speeds of CR fan, some acoustic benefits may be possible in its operating range.

For acoustics performance, under the same working point in the range of mid-high flow rate, the CR fan performs well and radiates lower noise than the series operation of small fans. However, it will generate more sound than the series operation when the volume flow rate decreases below the corresponding stall point. In other words, the CR fan functions best in the mid-to-high flow rate range, where the aeroacoustic advantage can be discovered. The CR fan working at lower rotational speeds is more environmentally friendly (lower SPL) and energy-efficient (lower rotational speeds) than the industrial fans operating in series in this flow rate range.

Beyond that, according to the noise spectra of the fan series and CR fan under approximately the same aerodynamic power point, it is obvious that the prominent tone frequencies are the integer multiples of the rear-rotor BPF and the linear combinations of both the front and rear rotor BPFs, meaning that the rear rotor radiates more noise and the interaction noise is primarily responsible for the tones of the CR fan. The tones of the CR fan do not form a large step like the fan series in the cumulative sound power curve since they spread over many peaks. On this account, the sound power is dispersive rather than the intensive tonal noise of the fan series. Therefore, the broadband noise is still the dominant noise contribution for the CR fan when compared to the fan series. With regard to the huge steps of the fan series, it is because the tonal radiation is enhanced and the tonal energy is larger than a single fan with the same rotating speed. The main contribution is the tonal noise and its control towards the broadband noise radiation is better than the CR fan. A good way to avoid tonal noise is to design a liner structure aiming at the most prominent tones and make the sound absorption band as wide as possible. However, due to the limitations of experimental conditions, the CR fan still needs improving for a fair comparison in the range from mid-to-high flow rate. For the follow-up work, the research on the aeroacoustic performance of the CR fan in the low flow rate range, namely near the stall point, will be the main object of study.

ACKNOWLEDGMENTS

The first author, Tianyu Xu, and the corresponding author, Bin Dong, would like to acknowledge the support from the University of Hong Kong, and China Aerodynamics Research and Development Center. Part of the work was also sponsored by the Natural Science Foundation of Sichuan Province (Grant No. 2023NSFSC0057).

REFERENCES

Peake, N., Parry, A.B. (2012), Modern challenges facing turbomachinery aeroacoustics, *Annu. Rev. Fluid Mech. 44* pp. 227-248.

Mitchell, G.A. and Mikkelson, D.C. (1982). Summary and recent results from the NASA advanced high-speed propeller research program. *18th Joint Propulsion Conference.*

Dong, B., Jiang, C., Liu, X., Deng, Y. and Huang, L.(2020). Theoretical characterization and modal directivity investigation of the interaction noise for a small contra-rotating fan. *Mechanical Systems and Signal Processing*, 135, pp.106362.

Dong, B., Xie, D., He, F. and Huang, L. (2021). Noise attenuation and performance study of a small-sized contra-rotating fan with microperforated casing treatments. *Mechanical Systems and Signal Processing*, 147, p.107086.

Dong, B., Zhao, Y., Tang, T. and He, F. (2023). Flow effects of microperforated-panel casing treatments in a contra-rotating fan. *International Journal of Mechanical Sciences*, 239, p.107879.

Jorgenson R. (1999), *Fan engineering: an engineer's handbook on fans and their applications*, Howden Buffalo Inc.

Wang C. (2018), Noise source analysis for two identical small axial-flow fans in series under operating condition, *Appl. Acoust*, 129, pp. 13-26.

Cho, L.-S., Cha, B.-J. and Cho, J.-S. (2009). Experimental Study on the Three-Dimensional Unsteady Flow Characteristics of the Counter-Rotating Axial Flow Fan. *Journal of Fluid Science and Technology*,4(1), pp.200–209.

Shigemitsu, T., Fukutomi, J. and Agawa, T. (2013). Internal Flow Condition of High Power Contra-Rotating Small-Sized Axial Fan. *International Journal of Fluid Machinery and Systems*, 6(1), pp.25–32.

Wang J., Ravelet F., Bakir F. (2013), Experimental comparison between a counter-rotating axial-flow fan and a conventional rotor-stator stage, *10th European Turbomachinery Conference*, Lappeenranta, Finland.

Chaitanya, P., Joseph, P., Prior, S.D. and Parry, A.B. (2022). On the optimum separation distance for minimum noise of contra-rotating rotors. *Journal of Sound and Vibration*, 535, p.117032.

Krause, R., Friebe, C., Kerscher, M. and Puhle, C. (2019). Investigations on noise sources on a contra-rotating axial fan with different modifications. *E3S Web of Conferences*, 111, p.02076.

AMCA (1999), *AMCA 210 Laboratory methods of testing fans for aerodynamic performance rating*, American Society of Heating, Refrigerating and Air-Conditioning Engineers, Washington.

Fukano, T., Takamatsu, Y. and Kodama, Y. (1986). The effects of tip clearance on the noise of low pressure axial and mixed flow fans. *Journal of Sound and Vibration*, 105(2), pp.291–308.

Lee, S. and J. Stuart Bolton (2016). Testing of axial fans with microperforated housings. *Noise Control Engineering Journal*, 64(4), pp.511–521.

Wang, C. and Huang, L. (2018). Theoretical Acoustic Prediction of the Aerodynamic Interaction for Contra-Rotating Fans. *AIAA Journal*, 56(5), pp.1855–1866.